

000 001 002 003 004 005 DYNAMIC MIXTURE EMBEDDINGS FOR CONTEXTUAL 006 META-REINFORCEMENT LEARNING 007 008 009

010 **Anonymous authors**
011 Paper under double-blind review
012
013
014
015
016
017
018
019
020
021
022
023
024

ABSTRACT

025 Contextual meta-reinforcement learning (meta-RL) relies on latent task embeddings
026 to enable rapid adaptation when faced with an unknown task. However, most
027 methodologies rely on unimodal priors, which lack the adaptive capacity to rep-
028 resent complex multimodal task structure, limiting performance when faced with
029 non-parametric variation. We introduce *Dynamic Mixture Embeddings (DME)*,
030 a belief-based contextual meta-RL method that learns a hierarchical Gaussian-
031 mixture Variational Autoencoder, in which mixture component parameters are
032 conditioned on a high-level macro latent. This yields an adaptive mixture prior
033 whose means and variances shift as more context is gathered, while training is fur-
034 ther augmented with virtual tasks drawn from the adaptive prior. DME achieves
035 state-of-the-art performance across the entire MetaWorld benchmark suite, de-
036 signed to test adaptation under non-parametric variation.
037

1 INTRODUCTION

038 Contextual meta-reinforcement learning (meta-RL) fundamentally seeks to endow an agent with the
039 ability to *infer the current task dynamics* after only a brief period of interaction, while retaining
040 strong performance across a broader task distribution. Functionally, this enables contextual meta-
041 RL policies to quickly adapt and re-optimize their behaviour when faced with new, unseen tasks.
042 Recent advancements in this field have produced a mature, practical framework that is seeing use
043 in a growing range of real-world systems, from robust autonomous driving in diverse environments
044 (Jiang et al., 2024; Hu et al., 2025) to situational behaviour in robotics applications (Ballou et al.,
045 2023; Shokry et al., 2024). Put together, these examples underscore meta-RL’s promise as a robust,
046 data-efficient alternative to task-specific reinforcement learning in scenarios with changing task dy-
047 namics.

048 The broad range of variations in environments and tasks a contextual meta-RL agent must face can be
049 separated, using the terminology of Yu et al. (2020), into two complementary groups. In *parametric*
050 *variation*, tasks differ only through continuous parameters such as limb mass, joint friction, reward
051 weights, or observation noise. While these variations still represent a broader distribution of MDPs,
052 contemporary algorithms are frequently able to attain near-expert performance after the handful of in-
053 teractions required to identify the task (Zintgraf et al., 2021b; Zhang et al., 2021). In *non-parametric*
054 *variation*, the structure and semantics of the task itself alters: object sets change, new goal interac-
055 tions appear, and the transition dynamics can change entirely. Although recent methods have taken
056 strides towards addressing these challenges through approaches such as task clustering (Chu et al.,
057 2024) and task simulation (Lee et al., 2023), empirical performance on key benchmarks remains
058 well below those achieved in the parametric setting.

059 As contextual meta-RL agents begin to tackle increasingly challenging problems, the representa-
060 tional capacity of latent embeddings that supply the agent with task context remains a bottleneck.
061 In complex environments, the complexity and variety of tasks can overwhelm an encoder’s ability
062 to separate qualitatively different behaviours and task regimes, leading to entangled representations
063 that blur the boundaries between objectives. At the same time, the encoder must remain flexi-
064 ble enough to account for previously unseen dynamics, while still maintaining the sample efficient
065 adaptation that underpins meta-RL as a whole. Addressing these requirements simultaneously is a
066 core challenge that motivates the methodology presented in this work.

054 A popular approach towards addressing some of these concerns involves multimodal representations
 055 with Gaussian mixture embeddings (Wen et al., 2024; Lee et al., 2023). By carving latent space
 056 into distinct regions, such embeddings are able to isolate incompatible modes of behaviour and
 057 therefore provide more representational capacity than standard Gaussian embeddings. However,
 058 existing methods suffer from rigidity in mixture parameters: the number and location of components
 059 are fixed *a priori*, so when training later encounters unexpected challenges, the model must choose
 060 an existing cluster, eroding representation quality and slowing adaptation.

061 We address this inflexibility with **Dynamic Mixture Embeddings** (DME), a contextual meta-RL
 062 method that utilises a hierarchical Gaussian-mixture variational auto-encoder (GMVAE) whose
 063 component parameters are themselves conditioned on a macro latent that is updated online from
 064 each context window. As new evidence arrives, mixture means and covariances migrate or expand,
 065 reallocating capacity while preserving previously learned structure. The primary contributions of
 066 our work are as follows:

- 067 1. We develop a task encoder based on a hierarchical Gaussian-Mixture VAE whose com-
 068 ponent parameters are conditioned on a macro latent variable. This dynamic mixture-
 069 representation not only achieves greater expressive capacity, but also integrates well with
 070 virtual training modules (Lee & Chung, 2021), strengthening robustness to non-parametric
 071 task variation.
- 072 2. The subsequent method, DME, achieves state of the art performance on the entire Meta-
 073 World benchmark suite (Yu et al., 2020), ranging from parametric variation in individual
 074 ML1 tasks, to the challenging non-parametric ML10 and ML45 benchmarks

076 2 PROBLEM STATEMENT AND NOTATION

079 In this section, we state the contextual meta-RL problem and align on notation for the rest of the
 080 paper. Each RL task can be considered as an MDP $M_i = \{S, A, P^i, R^i\}$ drawn from a distribu-
 081 tion $p(M)$. This distribution can contain both non-parametric and parametric task variation, but
 082 tasks from the same distribution are considered to be semantically similar and share some implicit
 083 structure across P^i and R^i . During adaptation, at timestep t the agent observes a short context
 084 $\mathbf{c}_{0:t} = \{(s_\ell, a_\ell, r_\ell, s_{\ell+1})\}_{\ell=0}^t$, and produces an episode-specific policy $\pi_\theta(a_t|s_t, \mathbf{c}_{0:t})$. For nota-
 085 tional simplicity, we will often drop the subscript t unless it is relevant (e.g. $\pi_\theta(a|s, \mathbf{c})$).

086 The meta-objective is to maximise expected return over the task distribution:

$$087 \max_{\theta} \mathbb{E}_{M_i \sim p(M)} \left[\mathbb{E}_{\tau \sim \pi_{\theta_i}} [r_i(\tau)] \right].$$

090 Finally, in this work we discuss a latent model with decomposition $z = (\tilde{w}, \tilde{y}, \tilde{z})$. Throughout this
 091 work, we will use z to represent latent representations as a conceptual whole, while \tilde{z} refers to the
 092 decomposed low-level task embedding.

094 3 RELATED WORK

096 **Contextual meta-RL.** Contextual meta-RL methods embed prior context into a probabilistic task
 097 representation, which in turn informs the RL policy, enabling rapid adaptation to new tasks. Tradi-
 098 tionally, contextual meta-RL methods have employed a single unimodal latent variable as the task
 099 representation (Zhao et al., 2021; Liu et al., 2021). Adaptation is typically achieved either by pos-
 100 terior sampling after a few exploratory episodes (Rakelly et al., 2019; Zhang et al., 2021; Wang
 101 et al., 2024), or by a belief-based approach in which task uncertainty is explicitly conveyed to the
 102 policy (Zintgraf et al., 2021a;b; Imagawa et al., 2022). While effective, such unimodal formulations
 103 can struggle to capture complex or multi-modal task distributions. Our approach, DME, takes a
 104 belief-based approach to adaptation but introduces a hierarchical mixture prior over latent variables,
 105 thereby providing a richer representational structure.

106 **Mixture latent variables and virtual training in meta-RL.** Gaussian mixture latent task
 107 representations have seen increasing use across all contextual meta-RL paradigms due to their ability

108 to model complex, multimodal task distributions. These mixture priors have been used to explicitly partition tasks for separate embedding modules (Chu et al., 2024), improve robustness in non-stationary environments (Poiani et al., 2021; Bing et al., 2023; Wang et al., 2023), and even extend the prior non-parametrically so the number of mixture components can grow (Bing et al., 2024).
 110 Compared to previous methods, DME conditions mixture component parameters on a high-level
 111 macro latent inferred from context, allowing means and variances to move during adaptation, as the
 112 inferred value of the macro latent is updated. Although hierarchical Gaussian mixtures have been
 113 considered in the broader meta-learning literature (Zhang et al., 2023), to our knowledge DME is
 114 the first to have truly adapted this dynamic latent structure to meta-RL.
 115

116 Virtual training augments these representations by simulating additional experience from learned
 117 task reconstructions. Within, task latents are sampled from the prior, before utilising a learned re-
 118 ward decoder to create simulated rewards, before attaching them to existing transitions to generate
 119 new context for training. This has been shown to be an effective mechanism to improve generalisa-
 120 tion beyond the empirical training task distribution across both on-policy (Lee & Chung, 2021; Lee
 121 et al., 2023; Kim et al., 2025).and off-policy (Ajay et al., 2022; Wen et al., 2024) variants. DME fol-
 122 lows the established template of sampling task latents and decoding rewards for stored transitions,
 123 but its synthetic tasks are drawn from adaptive mixture components, reducing dependence on tuning
 124 the number of mixtures K .
 125

126

127 **Hierarchical meta-RL.** Hierarchical control has long been used to tackle long horizons and
 128 hard exploration by decomposing behaviour across levels: a high-level controller proposes sub-
 129 behaviours or options and a low-level policy executes them (Bacon et al., 2017; Vezhnevets et al.,
 130 2017; Levy et al., 2017; Nachum et al., 2018). This abstraction seeks to concentrate exploration and
 131 credit assignment where it is most effective, utilising the slower decision-making time scales of the
 132 high-level controller to maintain consistent behaviour.

133

134 This policy-level hierarchy has also been adapted to the meta-RL problem through a variety of
 135 means. One approach abstracts sequences of actions into a stacks that are selected by a higher-level
 136 decision layer, seeking to standardise high-level choices across tasks and reduce the searchable task
 137 space during adaptation (Cho & Sun, 2024). Alternatively, instead of utilising action chains, addi-
 138 tional information can be provided to the hierarchical meta-RL agent, such as an action-conditional
 139 skill representation (He et al., 2024), or an auxiliary inner-loop value function (Bhatia et al., 2023).
 140 In both cases, the hierarchical structure has been shown to improve sample efficiency and generali-
 141 sation under task variation (Chua et al., 2023).

142

143 Our work takes an alternate route: instead of introducing a hierarchy of actions, DME builds hierar-
 144 chy into the task representation. By learning a dynamic, multi-level latent belief, DME can embed
 145 a wide collection of task representations in a similar fashion, while keeping a single policy that sees
 146 structured uncertainty in task inference. In this sense, DME aims to capture many of the benefits of
 147 hierarchy through latent representation rather than through a system of policies.

148

4 DYNAMIC MIXTURE EMBEDDINGS

149

150 Contextual meta-reinforcement learning (meta-RL) requires task embeddings that rapidly adapt
 151 while distinguishing related tasks. Adaptive mixture priors offer a principled route to handling
 152 diverse and complex tasks that require more flexibility than what traditional fixed mixture priors can
 153 provide. However, implementing these priors in a manner bespoke for contextual meta-RL is not
 154 trivial. Not only does training need to be structured in a way such to reduce the risk of overfitting
 155 the high-capacity latent hierarchy, but similar latent representations must also induce comparable
 156 behaviour in the policy.
 157

158

159 In this section, we introduce the key concepts underpinning our method DME. We begin by in-
 160 troducing the hierarchical Gaussian-mixture generative model at the core of DME, and discuss the
 161 training modules that integrate it into the contextual meta-RL process. From there, we describe the
 162 full DME algorithm and explain how virtual task simulation broadens the agent’s experience during
 163 training. Finally, we briefly summarise key implementation details.

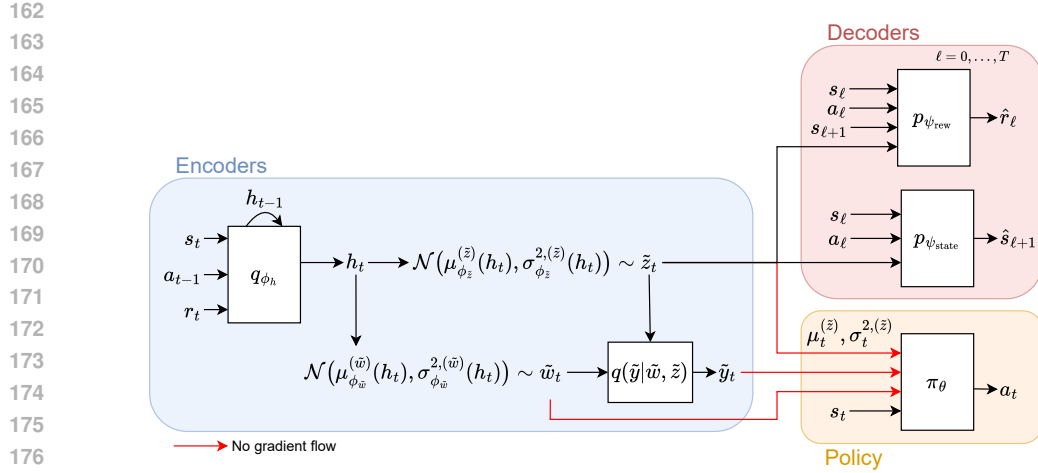


Figure 1: **DME overview.** Outline of a forward pass through DME and its hierarchical GMVAE encoder architecture. Online context is encoded into three latents: macro (\tilde{w}), mixture (\tilde{y}) and task (\tilde{z}). The RL policy utilises information from all three latents, including the task belief ($\mu^{(z)}, \sigma^{2,(z)}$). Only \tilde{z} is used in the decoders, ensuring that the lowest-level latent contains all information necessary to reconstruct the MDP.

4.1 HIERARCHICAL GAUSSIAN MIXTURE MODEL FOR DYNAMIC TASK EMBEDDINGS

Latent hierarchy. Inspired by the hierarchical variational model of Dilokthanakul et al. (2016), DME employs a three-tier latent structure $z = (\tilde{w}, \tilde{y}, \tilde{z})$. This consists of a continuous high-level macro-context latent $\tilde{w} \sim N(0, I)$ that dynamically controls mixture parameters, a discrete cluster latent $\tilde{y} \sim \text{Cat}(1/K)$ that partitions the task embedding space into semantically distinct regions, and a continuous low-level task embedding $\tilde{z}|\tilde{w}, \tilde{y} = k \sim N(m_\psi(\tilde{w}, k), v_\psi^2(\tilde{w}, k))$, where $k = 1, \dots, K$, that ultimately infers the specific task.

A decoder-side network parameterised by ψ maps the macro latent to mixture parameters, $\{(m_\psi(\tilde{w}, k), v_\psi^2(\tilde{w}, k))\}_{k=1}^K$, which define the component conditionals $p_\psi(\tilde{z}|\tilde{w}, \tilde{y} = k)$. The categorical \tilde{y} selects an index k ; given that index and \tilde{w} , \tilde{z} is drawn from the corresponding Gaussian. In this sense, the macro latent \tilde{w} parameterises the component Gaussians selected by \tilde{y} , determining in turn the means and variances of clusters in \tilde{z} -space. For the remainder of this section, we use ϕ for encoder parameters and ψ for decoder parameters.

Critically, this hierarchical structure is explicitly dynamic. The macro latent \tilde{w} actively repositions the Gaussian component means and variance structures in response to newly observed context. As a result, unlike the fixed cluster components learned by previous methods, mixture parameters naturally adapt and reallocate latent capacity in response to unseen task variation or distributional shift during training and testing.

Task posteriors. Unlike previous applications of this model - where training primarily seeks to fit observations drawn from a fixed generative prior - the objective of DME is to learn latent embeddings that quickly identify the underlying task given a small set of context transitions. Rather than shaping the prior to match observed data, the job of the variational model is to produce posteriors that capture sufficient task-relevant information to enable effective adaptation. Therefore, given the rolling context $\mathbf{c}_{0:t} = \{(s_\ell, a_\ell, r_\ell, s_{\ell+1})\}_{\ell=0}^t$, a recurrent encoder network parameterised by ϕ produces posterior distributions over the continuous latent variables:

$$q_\phi(\tilde{w}|\mathbf{c}_{0:t}) = N(\mu_\phi^{(w)}(\mathbf{c}_{0:t}), \sigma_\phi^{(w)2}(\mathbf{c}_{0:t})), \quad (1)$$

$$q_\phi(\tilde{z}|\mathbf{c}_{0:t}) = N(\mu_\phi^{(z)}(\mathbf{c}_{0:t}), \sigma_\phi^{(z)2}(\mathbf{c}_{0:t})). \quad (2)$$

Recurrent task encoders are utilised as they are better at exploiting temporal dependencies, which is a desirable property for on-policy meta-RL as it trains on sequential context.

Then, conditioning on inferred (\tilde{w}, \tilde{z}) , the discrete posterior for \tilde{y} can be computed analytically, avoiding high-variance gradient estimators:

$$q(\tilde{y} = k | \tilde{w}, \tilde{z}) = \frac{N(\tilde{z} | m_\psi(\tilde{w}, k), v_\psi^2(\tilde{w}, k))}{\sum_{j=1}^K N(\tilde{z} | m_\psi(\tilde{w}, j), v_\psi^2(\tilde{w}, j))}. \quad (3)$$

A low-variance estimator for the categorical cluster latent offers a crucial advantage over traditional neural estimators by keeping cluster assignments more stable during training, ensuring that downstream policy gradients are computed with minimal noise from label switching.

Parametrising the model this way reduces estimator variance and yields a single-path inference procedure: at test time, only the two Gaussian encoders $q_\phi(\tilde{w} | \mathbf{c}_{0:t})$ and $q_\phi(\tilde{z} | \mathbf{c}_{0:t})$ are required; the categorical $q(\tilde{y} | \tilde{w}, \tilde{z})$ is computed analytically, avoiding a separate network for \tilde{y} . Importantly, $q_\phi(\tilde{z} | \mathbf{c}_{0:t})$ is a single network, which mirrors the inference flow of unimodal methods such as VariBAD (Zintgraf et al., 2021a). However, DME’s training through its hierarchical generative model encourages \tilde{z} to take on a multimodal structure, retaining the benefits of mixture modelling without increasing inferential complexity at runtime.

At each timestep the encoder updates $q_\phi(\tilde{w} | \mathbf{c}_{0:t})$, $q_\phi(\tilde{z} | \mathbf{c}_{0:t})$, and the induced $q(\tilde{y} | \tilde{w}, \tilde{z})$ so the policy conditions on up-to-date beliefs rather than stale estimates.

Task Reconstruction. The low-level task embedding \tilde{z} is trained via an MLP decoder to best reconstruct *all future rewards and transitions*, not just at the current timestep. This coerces \tilde{z} to contain information that identifies the overall reward and transition function, allowing it to better reconstruct the true MDP. Concretely, sampling $\tilde{z}_t \sim q_\phi(\tilde{z} | \mathbf{c}_{0:t})$ from context-conditioned posterior, the decoder models the distribution over all future states and rewards

$$p_\psi(s_{t:T}, r_{t:T-1} | s_t, a_{t:T-1}, \tilde{z}_t) = \prod_{\ell=t}^{T-1} p_\psi(s_{\ell+1} | s_\ell, a_\ell, \tilde{z}_t) p_\psi(r_\ell | s_\ell, a_\ell, s_{\ell+1}, \tilde{z}_t), \quad (4)$$

where T denotes the end of the current episode horizon. Decoding the full rollout forces \tilde{z} to distil the information needed to recover the underlying task MDP dynamics and reward structure, rather than merely forecasting the next step, and provides the primary learning signal for the encoder–decoder.

Moreover, we choose to condition the decoder on \tilde{z} alone, excluding the macro \tilde{w} and cluster latent \tilde{y} . By omitting the higher-level variables from the reconstruction path we force the information bottleneck to reside in \tilde{z} , allowing \tilde{w} and \tilde{y} to play a predominantly organisational role and embed cluster information without entangling task dynamics across multiple latent representations.

Variational objective. With $\tilde{z}_t \sim q_\phi(\tilde{z} | \mathbf{c}_{0:t})$ and future indices $\ell \in \{t, \dots, T-1\}$, we introduce a prediction error for state and reward transitions as the primary training signal for our encoder:

$$\mathcal{L}_{\text{state}} = - \sum_{\ell=t}^{T-1} \log p_\psi(s_{\ell+1} | s_\ell, a_\ell, \tilde{z}_t), \quad (5)$$

$$\mathcal{L}_{\text{reward}} = - \sum_{\ell=t}^{T-1} \log p_\psi(r_\ell | s_\ell, a_\ell, s_{\ell+1}, \tilde{z}_t). \quad (6)$$

While predictive accuracy encourages precise information capture, we must also prevent latent embeddings from overfitting or completely collapsing into trivial forms. We assume independent priors $p(\tilde{w}) = N(0, I)$, $p(\tilde{y}) = \text{Cat}(1/K)$, and $p_\psi(\tilde{z} | \tilde{w}, \tilde{y}) = N(\mu_\psi(\tilde{w}, \tilde{y}), \sigma_\psi^2(\tilde{w}, \tilde{y}))$, and impose Kullback–Liebler (KL) constraints on each posterior:

$$\mathcal{L}_{\tilde{w}} = D_{\text{KL}}(q_\phi(\tilde{w} | \mathbf{c}) \| p(\tilde{w})), \quad (7)$$

$$\mathcal{L}_{\tilde{y}} = D_{\text{KL}}(q(\tilde{y} | \tilde{w}, \tilde{z}) \| p(\tilde{y})), \quad (8)$$

$$\mathcal{L}_{\tilde{z}} = D_{\text{KL}}(q_\phi(\tilde{z} | \mathbf{c}) \| p_\psi(\tilde{z} | \tilde{w}, \tilde{y})), \quad (9)$$

noting that the loss term for \tilde{y} has a closed-form solution.

Combining the predictive reconstruction and KL terms, we define our full variational training objective (ELBO) as

$$\mathcal{L}_{\text{ELBO}} = \alpha_s \mathcal{L}_{\text{state}} + \alpha_r \mathcal{L}_{\text{reward}} + \beta_w \mathcal{L}_{\tilde{w}} + \beta_y \mathcal{L}_{\tilde{y}} + \beta_z \mathcal{L}_{\tilde{z}}, \quad (10)$$

270 where $(\alpha_s, \alpha_r, \beta_w, \beta_y, \beta_z)$ are fixed loss coefficients.
 271

272 Intuitively, the reconstruction terms $(\mathcal{L}_{\text{state}}, \mathcal{L}_{\text{reward}})$ ensure task embeddings encode actionable information about present and future dynamics and rewards. The KL terms regularise the latent hierarchy:
 273 $\mathcal{L}_{\tilde{w}}$ centres the macro latent to minimise drift, $\mathcal{L}_{\tilde{y}}$ penalises deviation from a uniform categorical
 274 prior and encourages use of all clusters, while $\mathcal{L}_{\tilde{z}}$ aligns the encoder’s posterior $q_\phi(\tilde{z}|\mathbf{c})$ with the
 275 mixture prior $p_\psi(\tilde{z}|\tilde{w}, \tilde{y})$.
 276

277 **4.2 DYNAMIC MIXTURE EMBEDDINGS FOR CONTEXTUAL META-RL**
 278

279 DME leverages the hierarchical GMVAE architecture introduced in the previous section to infer latent
 280 task representations encountered in contextual meta-RL settings. Once learned, the full latent
 281 $z = (\tilde{w}, \tilde{y}, \tilde{z})$ can serve as an informative summary of task information, guiding the agent’s be-
 282 haviour in unseen tasks and environments. Pseudocode for the full DME algorithm can be found in
 283 the Appendix.

284 **Policy conditioning.** Following prior work in on-policy contextual meta-RL, we feed the policy
 285 the entire $\mu_{\tilde{z}}, \sigma_{\tilde{z}}^2$ posterior over the task latent \tilde{z} , rather than sampling a single inferred embedding
 286 (Zintgraf et al., 2021b). In Bayesian literature this constitutes the agent’s belief state, explicitly
 287 providing both the agent’s current estimate of the task and the uncertainty surrounding the estimate.
 288 Supplying the belief state allows the agent policy to decide dynamically whether to explore and
 289 reduce task uncertainty, or to exploit the existing prediction.

290 However, relying solely on \tilde{z} to influence agent behaviour provides little guidance about *where* in
 291 latent space would be most helpful to explore to reduce task uncertainty. Therefore, we also supply
 292 the policy with higher-level latents \tilde{w} and \tilde{y} . At every environment step the encoder revisits the
 293 accumulating context and refreshes its posteriors over \tilde{w}, \tilde{y} , and \tilde{z} . Together, they provide structured
 294 cues that accelerate adaptation and empirically improve performance in difficult benchmarks, as was
 295 seen in Section 5.2.

296 **Virtual training.** To improve robustness and generalisation, DME follows the lead of Lee et al.
 297 (2023) and employs virtual training, periodically generating synthetic tasks using its learned hierar-
 298 chical embedding and reward decoder. Virtual training seeks to address incomplete or insufficient
 299 task coverage by imagining plausible rewards for existing transitions under a different task embed-
 300 ding. These rewards are generated by sampling from the hierarchical prior:

$$\begin{aligned} \tilde{w}_{\text{virt}} &\sim p(\tilde{w}), \\ \tilde{y}_{\text{virt}} &\sim p(\tilde{y}), \\ \tilde{z}_{\text{virt}} &\sim p_\psi(\tilde{z}|\tilde{w}_{\text{virt}}, \tilde{y}_{\text{virt}}). \end{aligned}$$

305 Conditioned on the sampled virtual task representation \tilde{z}_{virt} , DME samples triplets $(s_\ell, a_\ell, s_{\ell+1})$
 306 from the replay buffer and produces a synthetic reward

$$r_{\text{virt}} \sim p_\psi(r | s, a, s', \tilde{z}_{\text{virt}}). \quad (11)$$

308 In practice, these synthetic trajectories are sampled alongside real experience at some scheduling
 309 rate $\gamma \in [0, 1]$, which is increased over time.
 310

311 **4.3 IMPLEMENTATION DETAILS**
 312

313 DME employs PPO (Schulman et al., 2017) as the base RL algorithm. The on-policy PPO naturally
 314 suits scenarios involving continuously evolving task embeddings \tilde{z} , since updating directly from
 315 recent trajectories avoids the distributional mismatches that arise in off-policy contexts.

316 Given the DME latent decomposition $z = (\tilde{w}, \tilde{y}, \tilde{z})$, the loss functions for training PPO with dy-
 317 namic mixture embeddings are given below

$$\rho_t = \frac{\pi_\theta(a_t | s_t, \tilde{w}_t, \tilde{y}_t, \tilde{z}_t)}{\pi_{\theta_{\text{old}}}(a_t | s_t, \tilde{w}_t, \tilde{y}_t, \tilde{z}_t)}, \quad (12)$$

$$\mathcal{L}_{\text{policy}} = -\mathbb{E}[\min(\rho_t A_t, \text{clip}(\rho_t, 1 - \epsilon, 1 + \epsilon) A_t)], \quad (13)$$

$$\mathcal{L}_{\text{value}} = \frac{1}{2} \mathbb{E}[(V_\theta(s_t, \tilde{w}_t, \tilde{y}_t, \tilde{z}_t) - \hat{V}_t)^2], \quad (14)$$

$$\mathcal{L}_{\text{entropy}} = -\beta_{\text{ent}} \mathbb{E}[\mathcal{H}(\pi_\theta(\cdot | s_t, \tilde{w}_t, \tilde{y}_t, \tilde{z}_t))]. \quad (15)$$

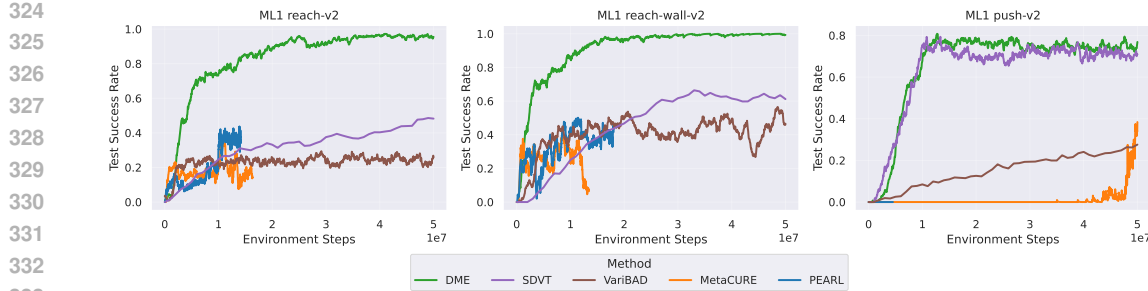


Figure 2: **MetaWorld ML1**. DME rapidly achieves near-perfect scores in the parametric single-environment MetaWorld ML1 benchmark, achieving a new state-of-the-art performance on those benchmarks.

where ρ_t represents the policy likelihood ratio, A_t is the advantage estimate and ϵ is the clipping constant.

The overall PPO loss,

$$\mathcal{L}_{\text{PPO}} = \mathcal{L}_{\text{policy}} + \mathcal{L}_{\text{value}} + \mathcal{L}_{\text{entropy}}, \quad (16)$$

is optimised separately from the variational objective, and we treat $(\tilde{w}, \tilde{y}, \tilde{z})$ as fixed conditioning variables (no gradient flow from \mathcal{L}_{PPO} to ϕ or ψ).

5 EXPERIMENTS AND RESULTS

In this section, we describe experiments that aim to answer the following questions: 1) How does DME adapt to parametric and non-parametric variation? 2) Does including the macro latent \tilde{w} in the policy input impact performance?

5.1 PARAMETRIC TASK ADAPTATION

Experiment setup. We begin by evaluating how well DME adapts to parametric task variation in order to understand whether DME’s flexible GMVAE parameterisation can efficiently adapt to a smaller potential task space. The MetaWorld ML1 benchmark consists of a variety of separate environments where a robotic Sawyer arm must complete a certain task. For this experiment, we choose *reach-v2*, *reach-wall-v2*, and *push-v2* due to their frequency in related works. Each ML1 environment randomises a variety of parameters at the start of the episode. The agent must infer those parameters from a handful of transitions and subsequently solve the task.

We compare DME against four strong contextual meta-RL baselines that range across both on-policy belief-based inference (like DME), and off-policy sample-based inference:

- variBAD (Zintgraf et al., 2021a), which shares the same core belief-based inference framework as DME but with a unimodal Gaussian task embedding.
- SDVT (Lee et al., 2023), which also utilises virtual training, but with a fixed-prior GMVAE.
- PEARL (Rakelly et al., 2019), an off-policy method that, after gathering context with an uninformative prior, samples a single fixed posterior task embedding per adaptation episode.
- MetaCURE (Zhang et al., 2021), which extends the PEARL method with a separate explorer that maximises task information gained during initial exploration.

For belief-based agents (DME, variBAD, SDVT) we measure the return and task success rates of the final (third) episode, while for sample-based agents (PEARL, MetaCURE) we provide two exploratory episodes and measure the performance of the subsequent exploitation episode. We utilise the original source code and hyperparameters for all implementations.

Results. Final success rates are presented in Figure 2. DME establishes a new state-of-the-art across the suite, achieving near-perfect success rates on *reach-v2* and *reach-wall-v2* in particular. On *push-*

v2, it performs similarly to its closest peer SDVT. This is not surprising - SDVT utilises a similar Gaussian mixture prior, but its structure is fixed. We hypothesise that the increased representational capacity enables the macro latent \tilde{w} to better learn the full range of parameterisation available, which allows the agent to completely solve the task.

Although the off-policy PEARL performs well in *reach-v2*, we note that wall-clock time for off-policy contextual meta-RL can be considerably longer due to the additional gradient steps taken per epoch. In addition, both PEARL and MetaCURE completely fail to solve *push-v2*, highlighting the fragility of their posterior sampling-based adaptation.

5.2 NON-PARAMETRIC TASK ADAPTATION

Experiment setup. Although parametric adaptation remains a relevant challenge in complex environments, the true challenge for contextual meta-RL algorithms lies in adapting to *non-parametric* task variation and the qualitatively different goals and transition dynamics that may result.

In order to evaluate the performance of DME when exposed to non-parametric task variation, we utilise the challenging MetaWorld ML10 and ML45 benchmarks, whose training environment sets span 10 and 45 distinct manipulation tasks, respectively. Each task corresponds to a separate ML1 environment - ranging from standard motion (*reach-v2*), to manipulation tasks (*door-open-v2*) and more unusual objectives (*basketball-v2*). Beyond these structural and semantic differences, each task also randomises continuous parameters (object masses, friction coefficients, goal positions), offering a comprehensive test of an algorithm’s capacity to adapt across both structural and parametric change.

After training, agents are evaluated on five held-out test tasks that were absent from the meta-training set but can, in principle, be solved by learning and applying the fundamental manipulation skills required to solve training tasks. We compare DME to the same peer baselines used in the parametric study — variBAD, SDVT, PEARL, and MetaCURE.

Results. Figure 3 reports success and return curves for both training and test tasks. Again, DME achieves the highest success rate on unseen test tasks, outperforming SDVT on both the ML10 and ML45 benchmarks. This improvement indicates that the ability to flexibly reallocate mixture means during training reduces over-specialisation and leaves extra capacity for genuinely novel behaviours.

This is further shown by how SDVT significantly outperforms DME in training environments, suggesting that the fixed mixture parameters of SDVT lead it to overfit on the training task distribution, leaving it unable to adapt to non-parametric task changes whose reward structure falls outside of its existing clusters. In contrast, the dynamic clusters of DME provide more capacity to generalise to unseen tasks at test time.

Only final results for the off-policy baselines, PEARL and MetaCURE, appear as they were tested for far fewer environment steps due to their off-policy nature. However, despite this, the wall-clock time remained comparable to the on-policy methods due to their tendency to take many more gradient steps per epoch. Despite this advantage in sample efficiency, both methods struggle to effectively adapt, possibly because their single-shot posterior sampling adaptation strategy is unreliable when needing to adapt to non-parametric changes in the task required.

5.3 ABLATION STUDIES

Policy input. Although the macro latent \tilde{w} is a crucial component of the hierarchical GMVAE, we seek to understand whether knowing \tilde{w} is helpful for the RL agent policy π_θ . We compare the full DME agent that passes \tilde{w} to the policy, $\pi_\theta(a|s, \tilde{w}, \tilde{y}, \tilde{z})$, to a variant that does not do so, resulting in the policy $\pi_\theta(a|s, \tilde{y}, \tilde{z})$. We continue to condition the policy on \tilde{y} as previous work has shown the benefits of including a discrete task- or subtask cluster as policy information (Lee et al., 2023).

In Figure 4, we see that conditioning on \tilde{w} consistently improves performance relative to the \tilde{w} -ablated variant across both *ML10* and *ML45* benchmarks. The intuition is straightforward: while \tilde{y} provides an explicit task cluster, the agent requires knowledge of the macro latent in order to understand where those clusters may be in embedding space. In this sense, both macro latent and cluster latent are required for the agent to truly understand mixture dynamics.

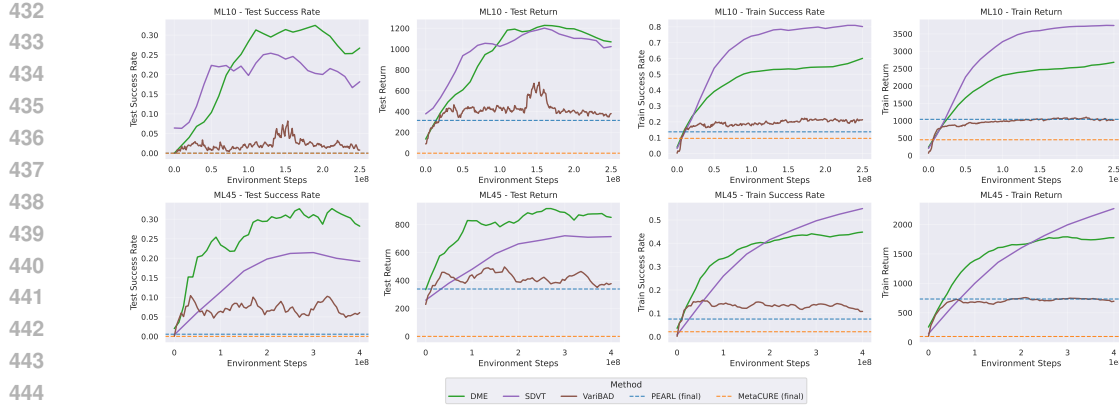


Figure 3: **Non-parametric MetaWorld.** DME outperforms contemporary contextual meta-RL methods on the difficult MetaWorld ML10 and ML45 benchmarks, achieving higher task success rates and returns. The lower success rates in training tasks suggest that DME’s adaptive clusters are less likely to overfit on the training distribution.

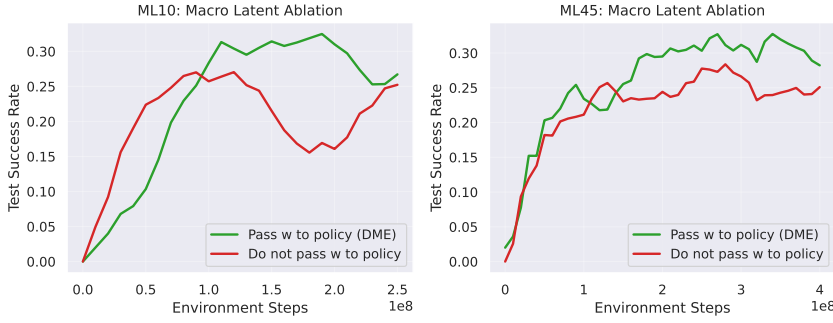


Figure 4: **Policy input ablation.** Passing the macro latent \tilde{w} to the meta-RL policy $\pi_\theta(a|s, \tilde{w}, \tilde{y}, \tilde{z})$ improves performance, suggesting that \tilde{w} contains information useful for adaptation.

6 CONCLUSION

In this paper we presented Dynamic Mixture Embeddings (DME), a contextual meta-RL algorithm that learns an adaptive Gaussian-mixture prior conditioned on a macro latent, so mixture components dynamically adapt as context is gathered. An analytic cluster assignment stabilises the hierarchy, while a decoder trained to predict entire future transitions and rewards pushes the continuous task code to capture MDP-level structure. Together, these choices deliver strong adaptation under both parametric and non-parametric variation, achieving state-of-the-art performance on the MetaWorld suite.

There are several promising directions for further study. First, there is still opportunity to investigate alternate formulations of the latent hierarchy, such as incorporating soft cluster assignments rather than relying solely on hard partitions. As this has proven successful in fixed-cluster context (Lee et al., 2023), we believe including the additional flexibility of DME-style may prove beneficial. In addition, there is certainly still room to refine the interaction between virtual training and the higher-level latents \tilde{w} and \tilde{y} . Integrating virtual training into cluster allocation or enabling dynamic cluster counts for \tilde{y} with a stick-breaking prior (Nalisnick & Smyth, 2017) could further improve the flexibility and robustness of this method.

Ultimately, this work has shown that dynamic hierarchical task representations are a practical and effective approach to improve adaptation and generalisation in contextual meta-RL. By utilising its adaptive mixture prior, DME demonstrates that representational flexibility matters for fast adaptation across both parametric and structural variation.

486 REFERENCES
487

488 Anurag Ajay, Dibya Ghosh, Sergey Levine, Pulkit Agrawal, and Abhishek Gupta. Distribution-
489 ally adaptive meta reinforcement learning. In *Decision Awareness in Reinforcement Learning*
490 *Workshop at ICML 2022*, pp. 25856–25869, New Orleans, USA, 2022.

491 Pierre-Luc Bacon, Jean Harb, and Doina Precup. The option-critic architecture. In *AAAI Conference*
492 *on Artificial Intelligence*, volume 31, San Francisco, USA, 2017.

493 Anand Ballou, Xavier Alameda-Pineda, and Chris Reinke. Variational meta reinforcement learning
494 for social robotics. *Applied Intelligence*, 53(22):27249–27268, 2023.

495 Abhinav Bhatia, Samer B Nashed, and Shlomo Zilberstein. RI3: Boosting meta reinforcement
496 learning via rl inside rl2. *arXiv preprint arXiv:2306.15909*, 2023.

497 Zhenshan Bing, David Lerch, Kai Huang, and Alois Knoll. Meta-reinforcement learning in non-
498 stationary and dynamic environments. *IEEE Transactions on Pattern Analysis and Machine*
499 *Intelligence*, 45(3):3476–3491, 2023.

500 Zhenshan Bing, Yuqi Yun, Kai Huang, and Alois Knoll. Context-based meta-reinforcement learning
501 with bayesian nonparametric models. *IEEE Transactions on Pattern Analysis and Machine*
502 *Intelligence*, 46(10):6948–6965, 2024.

503 Minjae Cho and Chuangchuang Sun. Hierarchical meta-reinforcement learning via automated
504 macro-action discovery. *arXiv preprint arXiv:2412.11930*, 2024.

505 Zhendong Chu, Renqin Cai, and Hongning Wang. Meta-reinforcement learning via exploratory task
506 clustering. In *AAAI Conference on Artificial Intelligence*, pp. 11633–11641, Vancouver, Canada,
507 2024.

508 Kurtland Chua, Qi Lei, and Jason Lee. Provable hierarchy-based meta-reinforcement learning. In
509 *International Conference on Artificial Intelligence and Statistics*, volume 206, pp. 10918–10967,
510 Valencia, Spain, 25–27 Apr 2023.

511 Nat Dilokthanakul, Pedro AM Mediano, Marta Garnelo, Matthew CH Lee, Hugh Salimbeni, Kai
512 Arulkumaran, and Murray Shanahan. Deep unsupervised clustering with gaussian mixture varia-
513 tional autoencoders. *arXiv preprint arXiv:1611.02648*, 2016.

514 Hongcai He, Anjie Zhu, Shuang Liang, Feiyu Chen, and Jie Shao. Decoupling meta-reinforcement
515 learning with gaussian task contexts and skills. In *AAAI Conference on Artificial Intelligence*,
516 volume 38, pp. 12358–12366, Vancouver, Canada, 2024.

517 Zechen Hu, Tong Xu, Xuesu Xiao, and Xuan Wang. Carol: Context-aware adaptation for robot
518 learning. *arXiv preprint arXiv:2506.07006*, 2025.

519 Takahisa Imagawa, Takuya Hiraoka, and Yoshimasa Tsuruoka. Off-policy meta-reinforcement
520 learning with belief-based task inference. *IEEE Access*, 10:49494–49507, 2022.

521 Yu Jiang, Kaixin Zhang, Minghao Zhao, and Hongde Qin. Adaptive meta-reinforcement learning for
522 auvs 3d guidance and control under unknown ocean currents. *Ocean Engineering*, 309:118498,
523 10 2024.

524 Jeongmo Kim, Yisak Park, Minung Kim, and Seungyul Han. Task-aware virtual training: Enhanc-
525 ing generalization in meta-reinforcement learning for out-of-distribution tasks. In *International*
526 *Conference on Machine Learning*, Vancouver, Canada, 2025.

527 Suyoung Lee and Sae-Young Chung. Improving generalization in meta-rl with imaginary tasks from
528 latent dynamics mixture. In *Advances in Neural Information Processing Systems*, volume 34, pp.
529 27222–27235, Virtual Conference, 2021.

530 Suyoung Lee, Myungsik Cho, and Youngchul Sung. Parameterizing non-parametric meta-
531 reinforcement learning tasks via subtask decomposition. In *Advances in Neural Information*
532 *Processing Systems*, New Orleans, USA, 2023.

540 Andrew Levy, George Konidaris, Robert Platt, and Kate Saenko. Learning multi-level hierarchies
 541 with hindsight. In *International Conference on Learning Representations*, Toulon, France, 2017.
 542

543 Evan Z Liu, Aditi Raghunathan, Percy Liang, and Chelsea Finn. Decoupling exploration and ex-
 544 ploration for meta-reinforcement learning without sacrifices. In *International Conference on*
 545 *Machine Learning*, pp. 6925–6935, Virtual Conference, 2021.

546 Ofir Nachum, Shixiang (Shane) Gu, Honglak Lee, and Sergey Levine. Data-efficient hierarchi-
 547 cal reinforcement learning. In *Advances in Neural Information Processing Systems*, volume 31,
 548 Montreal, Canada, 2018.

549 Eric Nalisnick and Padhraic Smyth. Stick-breaking variational autoencoders. In *International Con-
 550 ference on Learning Representations*, Toulon, France, 2017.

552 Riccardo Poiani, Andrea Tirinzoni, and Marcello Restelli. Meta-reinforcement learning by tracking
 553 task non-stationarity. In *International Joint Conference on Artificial Intelligence*, pp. 2899–2905,
 554 Montreal, Canada, 2021.

555 Kate Rakelly, Aurick Zhou, Chelsea Finn, Sergey Levine, and Deirdre Quillen. Efficient off-policy
 556 meta-reinforcement learning via probabilistic context variables. In *International Conference on*
 557 *Machine Learning*, pp. 5331–5340, Long Beach, USA, 2019.

559 John Schulman, Filip Wolski, Prafulla Dhariwal, Alec Radford, and Oleg Klimov. Proximal policy
 560 optimization algorithms. *arXiv preprint arXiv:1707.06347*, 2017.

561 Ahmed Shokry, Walid Gomaa, Tobias Zaenker, Murad Dawood, Rohit Menon, Shady A Maged,
 562 Mohammed I Awad, and Maren Bennewitz. Context-based meta reinforcement learning for robust
 563 and adaptable peg-in-hole assembly tasks. *arXiv preprint arXiv:2409.16208*, 2024.

565 Alexander Sasha Vezhnevets, Simon Osindero, Tom Schaul, Nicolas Heess, Max Jaderberg, David
 566 Silver, and Koray Kavukcuoglu. FeUdal networks for hierarchical reinforcement learning. In
 567 *International Conference on Machine Learning*, volume 70, pp. 3540–3549, Sydney, Australia,
 568 06–11 Aug 2017.

569 Min Wang, Xin Li, Leiji Zhang, and Mingzhong Wang. Metacard: Meta-reinforcement learning
 570 with task uncertainty feedback via decoupled context-aware reward and dynamics components.
 571 In *Proceedings of the AAAI Conference on Artificial Intelligence*, 2024.

573 Mingyang Wang, Zhenshan Bing, Xiangtong Yao, Shuai Wang, Kai Huang, Hang Su, Chenguang
 574 Yang, and Alois Knoll. Meta-reinforcement learning based on self-supervised task representation
 575 learning. In *AAAI Conference on Artificial Intelligence*, pp. 10157–10165, Washington, DC, USA,
 576 2023.

577 Lu Wen, Eric H. Tseng, Huei Peng, and Songan Zhang. Dream to adapt: Meta reinforcement
 578 learning by latent context imagination and mdp imagination. *IEEE Robotics and Automation
 579 Letters*, 9(11):9701–9708, 2024.

581 Tianhe Yu, Deirdre Quillen, Zhanpeng He, Ryan Julian, Karol Hausman, Chelsea Finn, and Sergey
 582 Levine. Meta-world: A benchmark and evaluation for multi-task and meta reinforcement learning.
 583 In *Conference on Robot Learning*, pp. 1094–1100, Cambridge, USA, 2020.

584 Jin Zhang, Jianhao Wang, Hao Hu, Tong Chen, Yingfeng Chen, Changjie Fan, and Chongjie Zhang.
 585 Metacure: Meta reinforcement learning with empowerment-driven exploration. In *International
 586 Conference on Machine Learning*, pp. 12600–12610, Virtual Conference, 2021.

587 Yizhou Zhang, Jingchao Ni, Wei Cheng, Zhengzhang Chen, Liang Tong, Haifeng Chen, and Yan
 588 Liu. Hierarchical gaussian mixture based task generative model for robust meta-learning. In
 589 *Advances in Neural Information Processing Systems*, volume 36, pp. 48662–48685, New Orleans,
 590 USA, 2023.

592 Zihao Zhao, Anusha Nagabandi, Kate Rakelly, Chelsea Finn, and Sergey Levine. Meld: Meta-
 593 reinforcement learning from images via latent state models. In *Conference on Robot Learning*,
 pp. 1246–1261, 2021.

594 Luisa Zintgraf, Sebastian Schulze, Cong Lu, Leo Feng, Maximilian Igl, Kyriacos Shiarlis, Yarin
 595 Gal, Katja Hofmann, and Shimon Whiteson. Varibad: Variational bayes-adaptive deep rl via
 596 meta-learning. *Journal of Machine Learning Research*, 22:1–39, 2021a.

597 Luisa M Zintgraf, Leo Feng, Cong Lu, Maximilian Igl, Kristian Hartikainen, Katja Hofmann, and
 598 Shimon Whiteson. Exploration in approximate hyper-state space for meta reinforcement learning.
 599 In *International Conference on Machine Learning*, pp. 12991–13001, Virtual Conference, 2021b.

600

601 **A APPENDIX: ALGORITHM**

602

603 **Algorithm 1 DME**

604

605 **Input:** Training task distribution $p(M)$, virtual rate γ
 606 Initialise on-policy storage B ; policy π_θ ; encoder q_ϕ ; decoder p_ψ
 607 **while** not done **do**
 608 Sample a task $M \sim p(M)$
 609 *# On-policy data collection*
 610 Reset context $\mathbf{c} \leftarrow \{\}$
 611 Sample $z_0 = (\tilde{w}_0, \tilde{y}_0, \tilde{z}_0) \sim p(\tilde{z}|\tilde{y}, \tilde{w})p(\tilde{y})p(\tilde{w})$
 612 **for** timestep t during rollout **do**
 613 Form policy belief $b_t = (\mu_{\tilde{z}_t}, \sigma_{\tilde{z}_t}^2, \tilde{w}_t, \tilde{y}_t)$
 614 Sample action $a_t \sim \pi_\theta(a_t|s_t, b_t)$ and step environment
 615 Append (s_t, a_t, s_{t+1}, r_t) to B and update $\mathbf{c}_{0:t}$
 616 Update $z_{t+1} = (\tilde{w}_{t+1}, \tilde{y}_{t+1}, \tilde{z}_{t+1}) \sim q_\phi(\tilde{w}|\mathbf{c}_{0:t})q_\phi(\tilde{z}|\mathbf{c}_{0:t})q(\tilde{y}|\tilde{w}, \tilde{z})$
 617 **end for**
 618 *# Training steps*
 619 Sample minibatches of sequential context $\mathbf{c} \sim B$ and an on-policy PPO batch $\mathbf{x} \sim B$
 620 Re-calculate posterior $z = (\tilde{w}, \tilde{y}, \tilde{z}) \sim q_\phi(\tilde{w}|\mathbf{c})q_\phi(\tilde{z}|\mathbf{c})q(\tilde{y}|\tilde{w}, \tilde{z})$
 621 Calculate $\mathcal{L}_{\text{state}}$ according to Equation 5
 622 **if** with probability γ **then**
 623 *# Virtual update*
 624 Sample $(\tilde{w}_{\text{virt}}, \tilde{y}_{\text{virt}}, \tilde{z}_{\text{virt}}) \sim p(\tilde{z}|\tilde{y}_{\text{virt}}, \tilde{w}_{\text{virt}})p(\tilde{y})p(\tilde{w})$ from prior
 625 Calculate rewards r_{virt} according to Equation 11
 626 Calculate $\mathcal{L}_{\text{reward}}$ using virtual rewards
 627 **else**
 628 Calculate $\mathcal{L}_{\text{reward}}$ according to Equation 5
 629 **end if**
 630 Calculate $\mathcal{L}_{\tilde{w}}$, $\mathcal{L}_{\tilde{y}}$, $\mathcal{L}_{\tilde{z}}$ according to Equations 7-9
 631 Calculate $\mathcal{L}_{\text{ELBO}}$ according to Equation 10
 632 Calculate \mathcal{L}_{PPO} according to Equation 16
 633 *# Gradient update*
 634 Update ψ, ϕ by minimising $\mathcal{L}_{\text{ELBO}}$
 635 Update θ by minimising \mathcal{L}_{PPO}
 636 Empty B
 637 **end while**

638

639

640

641

642

643

644

645

646

647